Anisotropy, multivalency and flexibility-induced effects in colloidal systems
Verweij, R.W.

Citation
Verweij, R. W. (2021, May 27). *Anisotropy, multivalency and flexibility-induced effects in colloidal systems*. *Casimir PhD Series*. Retrieved from https://hdl.handle.net/1887/3179461

Cover Page

Universiteit Leiden

4 Linker-mediated interactions among colloid-supported lipid bilayers

I N biological systems, adhesion is commonly mediated by multivalent interactions of multiple ligands and receptors, for example in the attachment of viruses to host cells and in cell signaling processes. Additionally, multivalent interactions are a promising way to control the self-assembly of synthetic materials, for example in colloidal systems. Here, we have used optical tweezers to directly probe the binding probability of DNA-decorated colloid-supported lipid bilayers as function of DNA linker concentration and valency. We have quantified the effect of linker depletion, where binding multiple 'guest' particles to the same 'host' particle that has a fixed linker concentration leads to a decrease in the binding probability. Using these results, we predict the dependence of the expected valency in self-assembly experiments on the linker concentration and compare this to preliminary experimental data. Beyond applications for colloidal self-assembly processes, our findings could have implications for multivalent interactions found in biological systems, such as in cell-signaling and drug-delivery systems.

4.1   Introduction

In biological systems, attractive interactions are commonly mediated by multiple ligands and receptors that have a specific affinity for each other, for example in the attachment of viruses to the membrane of host cells.[232] Moreover, these multivalent interactions also play a large role in cell signaling processes.[233–235] While the individual interactions between ligands and receptors are often weak, the number of formed bonds amplifies the overall adhesive strength, leading to large bonding energies with a high affinity for the target structures.[235] A complete understanding of these multivalent interactions could lead to significant advances in targeted drug delivery, where fine-grained control over the type of cells a drug acts on is called for.[7–9,114–117] In drug-delivery systems, both nanoparticle- and microparticle-based systems are used. While both classes of particles have useful applications, significant advantages of microparticles over nanoparticles are their higher loading capacity,[7] their lower biotoxicity because of their inability to cross biological membranes[6,8,115] and simpler production and characterization methods. Therefore, microparticle-based drug delivery systems show great promise to provide new therapies to a wide range of diseases.[7,8]

Beyond biological and medical applications, multivalent interactions are a promising route to providing full control over self-assembly processes in material science,

for example by using microparticles functionalized with DNA linkers.[4,70–76] There, the specificity of the Watson-Crick base paring has been used to synthetically construct pieces of single-stranded DNA that specifically hybridize with each other and therefore can act as an "intelligent glue" between the micron-sized colloidal particles. These developments triggered efforts to employ DNA-coated colloids as building blocks for materials with highly sought after properties, such as photonic bandgaps.[71]

Theoretical and experimental studies on multivalent interactions in systems of DNA-coated colloids have revealed their great potential for applications and their rich behavior, in which entropic effects were found to play a dominant role.[50,73,75,236–240] Namely, the entropic contributions of the DNA linkers to the free energy were found to be of similar magnitude as the hybridization free energy of a pair of sticky ends.[73] Entropic contributions to the free energy of the system can stem, for example, from the reduction in the configurational entropy of the linkers upon binding,[73,237,240] from entropic repulsion between linkers (and/or surfaces) because of excluded volume interactions,[73,229,240] from the combinatorial entropy gain originating from the possible combinations of forming bonds between a given number of linkers,[73,229] or from the loss in configurational entropy when surface-mobile linkers are confined to the contact area between two bound particles.[240] Additionally, the distribution of DNA linkers on the surface was shown to lead to large variations in binding strength.[73] The interactions between DNA-coated colloids were found to be further modifiable by, for example, changing the ionic strength of the solution, or by including inert DNA strands that alter only the repulsive part of the free energy.[236] These examples are not fully comprehensive, but serve to illustrate both the complexity and the rich potential of DNA-mediated interactions.

Typically, because of the combination of the high binding strength, narrow melting temperature range and slow binding kinetics[50] of DNA-mediated interactions, most DNA-coated colloids were found to kinetically arrest into amorphous structures, except if patchy particles were used[2] or by employing high coating densities of short DNA linkers consisting of a few basepairs.[241] Another proposed way to overcome the effects of kinetic arrest is to employ colloidal particles where the DNA linkers can freely diffuse on the particle surface, using colloid-supported lipid bilayers[85,110,112,242] (CSLBs). CSLBs consist of solid colloidal particles that are coated with a fluid lipid bilayer, into which DNA linkers with a hydrophobic anchor can be inserted. Because of the fluidity of the bilayer, the DNA linkers can surf over the particle[110,112] and the resulting self-assembled structures can rearrange with respect to each other,[85,242] thereby overcoming equilibration issues caused by kinetic arrest.

While, as discussed, the interactions between DNA-coated colloids containing grafted DNA linkers have been extensively studied, less is known about the effect of mobile DNA linkers. Experimentally, their binding probability as function of temperature was characterized[110] and broad association/dissociation transitions were found for a range of DNA concentrations. In theoretical studies, it was shown that it should be possible to control the valency, i.e. the number of binding partners, of colloids

with mobile linkers by tuning the amount of nonspecific repulsion.[229] Another theoretical work found that when the rate at which bonds are formed is low with respect to the particle diffusion coefficient, the average valency can be controlled.[243] Linker depletion effects, that also lead to a slow down of the self-assembly process, were observed in the adhesion of nanoparticles to lipid membranes[126] and in systems of DNA linker-functionalized emulsion droplets.[84] These results taken together demonstrate that by using colloidal particles decorated with mobile DNA linkers, precise control over the valency of the particles, and therefore over the formed structures, should be within reach.

Here, we study linker depletion effects in a system of CSLBs as a means to control the average valency in self-assembly experiments. First, we measure the binding probability of CSLBs as function of DNA concentration. In addition, we asses the effect of the sequential assembly of particles onto a central particle. In this way, we experimentally quantify the effect of nonspecific repulsion, specific attraction and linker depletion effects. We provide an outlook of possible applications of our findings to colloidal self-assembly. Beyond that, our findings could have implications for multivalent interactions found in biological systems, such as in cell-signaling and drug-delivery systems.

4.2   Materials and Methods

4.2.1   Particle coating

Colloid-supported lipid bilayers (CSLBs) were prepared as described in previous work,[85,110,112,242,244] specifically, we followed a similar procedure as in chapters 3 and 5. First, we prepared small unilamellar vesicles (SUVs) consisting of 98.9 mol % of the unsaturated phospholipid DOPC ((Δ9-Cis)-1,2-dioleoyl-sn-glycero-3-phosphocholine), 1 mol % of the lipopolymer DOPE-PEG(2000) (1,2-dioleoyl-sn-glycero-3-phosphoethanolamine-N-[methoxy-(polyethylene glycol)-2000]) and 0.1 mol % of the dyed lipids TopFluor-Cholesterol (3-(dipyrrometheneboron difluoride)-24-norcholesterol) or alternatively, DOPE-Rhodamine (1,2-dioleoyl-sn-glycero-3-phosphoethanolamine N-(lissamine rhodamine B sulfonyl)), where we matched the fluorescent dyes of the lipids and linker DNA. Specifically, we used 77 μL of DOPC ($25\,\mathrm{g\,L^{-1}}$), 7.3 μL of DOPE-PEG(2000) ($10\,\mathrm{g\,L^{-1}}$) and 3.4 μL of the fluorescent lipids ($1\,\mathrm{g\,L^{-1}}$). The lipids in chloroform were mixed and dried in a vacuum desiccator for 2 h in a glass vial. Then, 4 mL of a buffer at pH 7.4 containing 50 mM sodium chloride (NaCl) and 10 mM 4-(2-Hydroxyethyl)-1-piperazineethanesulfonic acid (HEPES) was added. The dispersion was mixed using a vortex mixer for 45 min. SUVs were prepared using an Avanti Mini Extruder by extruding the dispersion 21× through a 50 nm pore-size polycarbonate membrane supported by two filter supports.

Next, the (2.12 ± 0.06) μm silica particles obtained from MicroParticles GmbH were washed in water. The particles were coated with a fluid lipid bilayer by deposition and rupture of SUVs by mixing 200 μL of the 50 mM HEPES buffer, 23 μL of the SUVs and 100 μL of the silica particles (0.05 %w/w). This mixture was rotated for
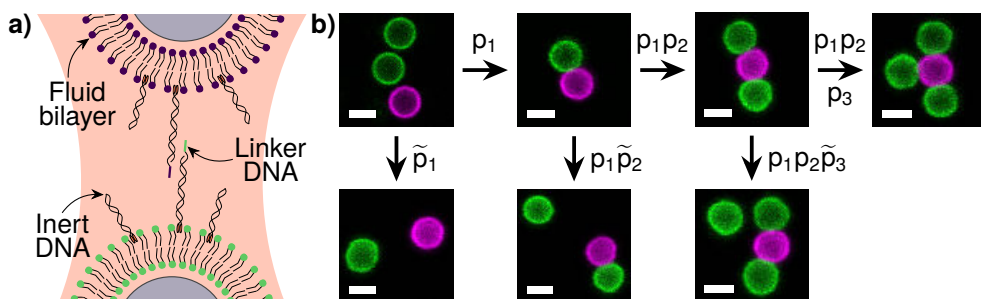
Figure 4.1: **Experimental system. a)** Two CSLBs decorated with complementary linker DNA are brought into close proximity using optical tweezers to facilitate DNA-mediated binding. In addition to linker DNA, we have added inert DNA that does not have a sticky end but provides additional steric repulsion and therefore improves colloidal stability. The fluid lipid bilayer allows the DNA to diffuse on the surface of the particles. **b)** After releasing the trap, the particles can either bind or not. We show confocal images of all tested cases with their associated probabilities p_n and negated probabilities $\widetilde{p}_n$. In this way, we performed a sequence of Bernoulli trials until a valency n of up to three bonded particles to the central particle (here, in purple) was reached. We waited for at least 5 min between consecutive trials and discarded the cluster when a trial was unsuccessful. Scale bars are 2 μm.

30 min. Afterwards, the mixture was washed once in HEPES buffer solution in order to remove excess SUVs.

We added double-stranded DNA (of respectively strands DS-H-A and DS-H-B, see Table A.1) with an 11 base pair long sticky end and a double stearyl anchor, which inserts itself into the bilayer via hydrophobic interactions, as shown Figure 4.1a. The sticky end of strand DS-H-A is complementary to the sticky end of strand DS-H-B, which allows them to act as linkers. For additional steric stabilization without adding additional linkers, we have added double-stranded inert DNA with a double stearyl anchor (strand DS-H-I in Table A.1). The length of the inert DNA is approximately 20 nm and the linker DNA length is 30 nm. We tested various concentrations of both inert and linker DNA. All DNA solutions were prepared using a buffer of pH 7.4, containing 200 mM NaCl and 10 mM HEPES, which we call the 200 mM HEPES buffer. Buffers and DNA solutions were freshly prepared in the same week as the experiment, to prevent degradation of the hybridized DNA that happens over time. After adding the required amounts of DNA to the particles, the mixture was rotated for 1 h. Then, it was washed three times in 200 mM HEPES buffer. For imaging, we used a metal sample holder containing a polyacrylamide (PAA) coated cover glass.[244] Confocal microscopy images of the coated particles are shown in Figure 4.1b. All solutions were prepared with ultra pure Milli-Q water (Milli-Q Gradient A10).

4.2.2 Microscopy and binding experiments

Imaging was performed using an inverted confocal microscope (Nikon Eclipse Ti-E) equipped with a Nikon A1R confocal scanhead with galvano and resonant scanning mirrors. A 60× water immersion objective (NA=1.2) was used. 488 and 561 nm lasers were used to excite, respectively, the TopFluor and Rhodamine dyes. Laser emission passed through a quarter wave plate to avoid polarization of the dyes and the emitted light was separated by using $500 - 550\,nm$ and $565 - 625\,nm$ filters.

We used optical tweezers to probe the binding probabilities. Briefly, we employed a homemade optical setup consisting of a highly focused trapping laser manufactured by Laser QUANTUM (1064 nm wavelength). The laser beam entered the confocal microscope through the fluorescent port, after first passing through a beam expander and a near-infrared shortpass filter. The same objective was used for imaging and to focus the trapping laser beam. During the trapping, the quarter wave plate was removed from the light path. The temperature of the sample was controlled using a water-cooled sample stage set at 20 °C.

We are interested in testing the binding probability as function of valency n, or the total number of binding partners, as depicted in Figure 4.1b. To probe the binding probability, two complementary particles were trapped using a trap strength of 75 to 150 mW for 30 s. The trapping strength was determined empirically, by testing the power that was just enough to lift a particle from the substrate. We then multiplied the obtained value by a factor of two and repeated this procedure of calibrating the trapping strength for each set of experiments. After 30 s of trapping two particles, the trap was released. If particles remained bonded, we tested whether they were indeed permanently bound by gently pulling on one of the particles using the optical tweezers. We then counted all pairs of particles that were either bound or not. After waiting for at least 5 min, we repeated the experiment by trying to add another particle, while ensuring that enough time had passed after binding for the binding patch of bonded linker DNA to fully develop. This was repeated until the particles would either not bind, or a valency $n = 3$ was reached, as depicted in Figure 4.1b. In this way, we performed a sequence of Bernoulli trials using the same cluster, which implies that the amount of DNA on the central particle is expected to be the same for the different trials, allowing for a direct comparison of the binding probabilities as function of valency.

4.2.3 Self-assembly experiments

In addition to the optical tweezers experiments, we have performed self-assembly experiments, in which two sets of CSLBs functionalized with complementary DNA linkers were mixed at a high number ratio of 'host' to 'guest' particles of 1:30. This high number ratio drives the self-assembly process towards the formation of clusters,[85] as opposed to other structures such as chains and fractal aggregates. The particles were mixed in the 200 mm HEPES buffer and put into a metal sample holder containing a PAA coated cover glass[244] at a particle concentration of approximately 2×10^{-4} % w/v.

The effective particle area density in the experiment was larger, because the particles were confined to the substrate by sedimentation. Then, the distribution of clusters was counted at several instances in time, where we recorded the number of clusters per valency, the number of nonspecific aggregates and the number of clusters that we could not ascribe a valency to, such as chains or fractal aggregates. For each measurement, at least 100 clusters were counted. The average valency we report here was determined after at least 24 h of mixing. After that time, we found that the average valency did not increase further.

4.2.4 Data analysis

The experimental binding probabilities p_n were determined from the number of bound and unbound particles by calculating a binomial proportion confidence interval, specifically, the Wilson score interval,[245]

$$p_n \pm \sigma_n = \frac{N_B + \frac{1}{2}z^2}{N_T + z^2} \pm \frac{z}{N_T + z^2} \sqrt{\frac{N_B N_U}{N_T} + \frac{z^2}{4}}, \tag{4.1}$$

where n is the valency, σ_n the estimated error on p_n, N_T the total number of particles tested, N_B is the number of trials that resulted in bonded particles, N_U is the number of trials where bonding failed and $z = 1$ such that we report one standard deviation. Fits to the experimental data were performed using a standard least-squares method as implemented in the Python package `lmfit`[246] and we report one standard deviation calculated using the `conf_interval` function.

4.3 Results and Discussion

4.3.1 DNA-mediated interactions between CSLBs

We experimentally probe the binding probability of DNA-functionalized colloid-supported lipid bilayers[85,110,112,242] (CSLBs). The CSLBs consist of spherical colloidal silica particles, that are surrounded by a fluid lipid bilayer. DNA linkers with complementary sticky ends are inserted into the bilayer using a hydrophobic anchor. The particles are self-assembled by hybridization of the DNA sticky ends, which provide strong and specific interactions. A fraction of the DNA strands, which we call inert DNA strands, do not contain a sticky end and therefore only contribute to the repulsive part of the interaction between two CSLBs. The resulting particle assemblies can rearrange with respect to each other, because the DNA linkers can diffuse on the fluid lipid bilayer that surrounds the particles, as shown in Figure 4.1a. To experimentally measure the probability of binding, we use optical tweezers to bring specific particles into close contact for a controlled amount of time. This allows us to probe the binding probability as function of DNA linker and inert concentration and as function of the valency of the binding partners. Specifically, we test the ability of a particle to bind to one to three particles in a sequential fashion, as shown in Figure 4.1b. A sequence of Bernoulli trials is conducted, where we first try to bind two complementary particles.

If this succeeds, we wait for at least 5 min to allow a DNA linker patch to form between the bonded particles. Then, we try to bind another particle to obtain a valency $n = 2$ and, after a second 5 min waiting period, a third particle so that we obtain a final valency $n = 3$, as depicted in Figure 4.1b.

Suppressing nonspecific interactions

The binding probability can only be accurately measured if nonspecific interactions between the particles are suppressed. To quantify the fraction of particles that bind via interactions not mediated by the DNA linkers, we first probe the binding probability of CSLBs that have no linker DNA or are functionalized with the same type of linker DNA, that is not self-complementary and therefore cannot form bonds. In our previous work[242] in Chapter 3, we have found that nonspecific interactions can be suppressed by increasing the concentration of inert DNA. There, we did not use optical tweezers to test the binding probability, but instead calculated the ensemble average by counting the fraction of bound particles after a given equilibration period of a few hours. The method that uses optical tweezers is a more direct and more controlled way of measuring the binding probability of two particles, because it allows for more control over both the duration of close contact and the applied force.

Surprisingly, as shown in Figure 4.2a, the probability to form nonspecific aggregates determined from the counting method differs strongly from the probability determined using the optical tweezers based method. By probing the fraction of particles that form nonspecific aggregates using optical tweezers, we find a lower fraction for CSLBs without DNA linkers of 0.33 ± 0.04 compared to 0.65 ± 0.08 using the counting method. Additionally, using the tweezers, we find that low concentrations of DNA already greatly suppress nonspecific interactions. While there is still a significant fraction of nonspecific aggregates at concentrations of $10^4\,\mu m^{-2}$ as determined from the counting method, when we probe the probability to form nonspecific aggregates using the tweezers, we find that they are almost completely absent for those DNA concentrations. Therefore, we conclude that after the functionalization with DNA of a sufficiently high concentration of approximately $10^4\,\mu m^{-2}$, nonspecific aggregations are completely suppressed. The discrepancy between the counting and tweezers methods implies that the aggregates that were observed using the counting method were formed before the DNA was added, most likely during the stage where the bilayer was formed on the particles using the deposition and rupture of small vesicles. Additionally, the counting method could slightly overestimate the number of clusters: as the number of clusters was determined automatically from (static) images, particles were already considered to be part of a cluster when their separation distance was smaller than 2.2 times the particle radius, as explained in detail Section 3.2.6. As shown in Figure 4.2b, increasing either the linker or inert DNA concentration leads to a decrease in nonspecific aggregation, as visualized in the confocal microscopy images.

This observation indicates that further improvements to the coating scheme may be possible. For example, using lower concentrations of salt during the bilayer coat-
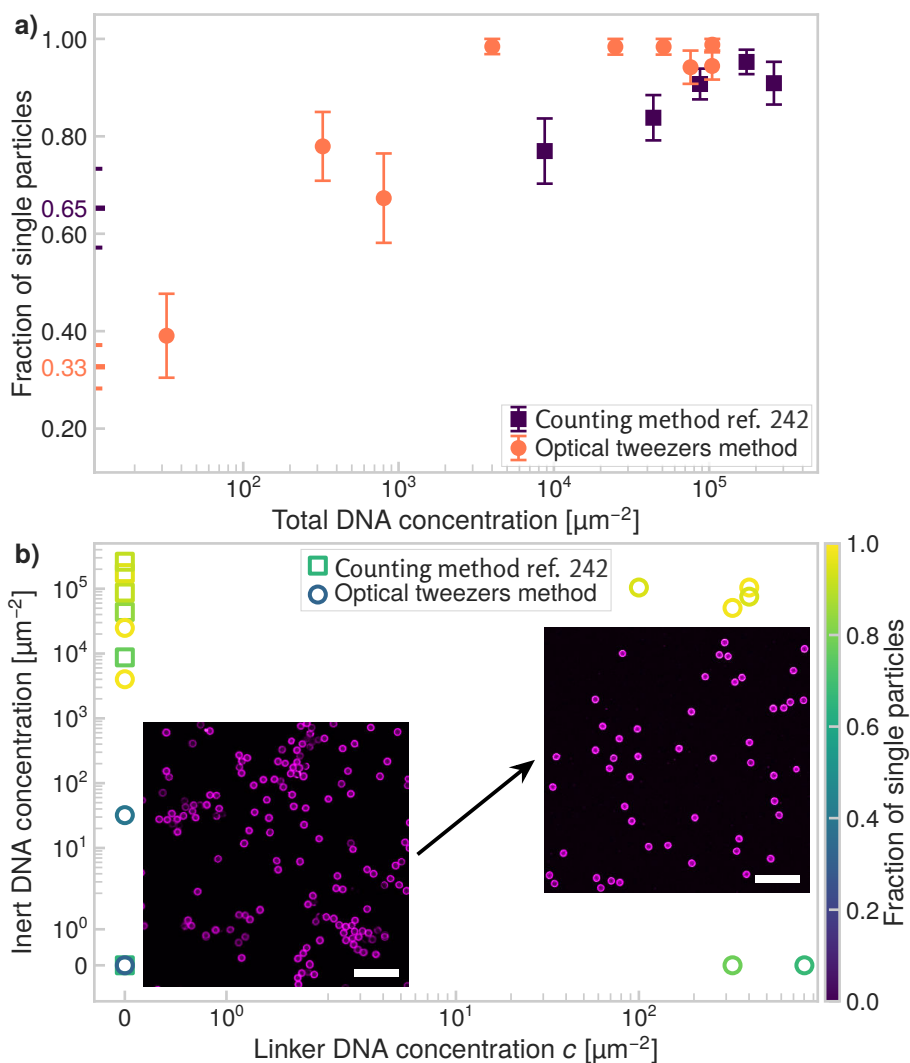
Figure 4.2: **Suppressing nonspecific interactions.** Increasing the amount of either linking or inert DNA reduces nonspecific binding, our tweezers based method reproduces earlier results obtained by counting random aggregates.[242] **a)** Fraction of single particles as function of the total amount of added DNA in terms of the surface density of both inert and linker DNA. Colored ticks indicate the fraction of single particles if no DNA is added. **b)** Plot of the fraction of single particles (color scale) as function of inert DNA and linker DNA concentration. As shown in the confocal images, randomly-bonded aggregates are frequently observed when the total DNA concentration is low (lower left), in contrast to the large percentages of single particles for sufficiently high DNA concentrations (upper right). Scale bars are 15 µm.

ing phase should slow down the formation of nonspecific aggregates by increasing the Debye screening length. In preliminary experiments, we have found that ionic strengths of approximately 15 mM are sufficient to promote the rupture and spreading of vesicles on the particle surface. Additionally, the relative concentrations between vesicles and particles should be carefully tuned. High concentrations of vesicles could induce depletion interactions that would result in nonspecific aggregation of the particles. We have found that a surface ratio between particles and SUVs close to 1:10 strikes a good balance between low vesicle concentrations and homogeneous bilayer formation.[242] In future experiments, the colloidal stability during the bilayer coating should be studied in more detail. Importantly, we conclude that these measurements show that spontaneous destabilization in an assembled structure is unlikely when the total DNA concentration exceeds $10^4\,\mu m^{-2}$.

Experimental binding probability

Having found the lowest DNA concentration of $10^4\,\mu m^{-2}$ that still provides sufficient colloidal stability, we now characterize the binding probability p_1 of binding a pair of CSLBs. We have varied both the inert and linker DNA concentrations. Indeed, we observe again that when no inert DNA is added, the binding probability p_1 of forming a dimer is high even if no linker DNA is added, as shown in Figure 4.3a. More importantly, when inert DNA is added for stability, we observe an S-shaped increase in the binding probability as function of DNA linker concentration, as can be seen in Figure 4.3a. Furthermore, we note that for the lower inert DNA concentration $(0.5 \times 10^5\,\mu m^{-2})$, the transition from no binding to binding is shifted towards larger linker concentrations compared to the higher inert DNA concentration $(1 \times 10^5\,\mu m^{-2})$. For the higher valencies $n = 2$ and 3 shown in, respectively, Figure 4.3b and c, there is a qualitative difference between the two inert DNA concentrations: for the high one $(1 \times 10^5\,\mu m^{-2})$, we observe very similar binding curves for all valencies. For the lower inert DNA concentration $(0.5 \times 10^5\,\mu m^{-2})$, we note that the transition between no binding and binding is broadened as function of valency and is shifted towards larger linker concentrations as the valency increases.

Linker depletion as function of valency

This shift towards higher linker concentrations hints at a linker depletion effect. Because the amount of DNA strands on any given particle is fixed, it is reasonable to assume that for each additional 'guest' particle that binds to a given 'host' particle, the concentration of available linkers on the host particle decreases. This effect, known as linker depletion, has previously been observed in experiments where nanoparticles decorated with linkers were bound to lipid membranes[126] and in the self-assembly of DNA-functionalized emulsion droplets.[84] This mechanism of linker depletion is interesting because it could be exploited to limit the valency of colloidal clusters in self-assembly experiments.

We would like to model the observed behavior, in order to extract quantitative trends from our experimental measurements. So far, it has been proven challenging
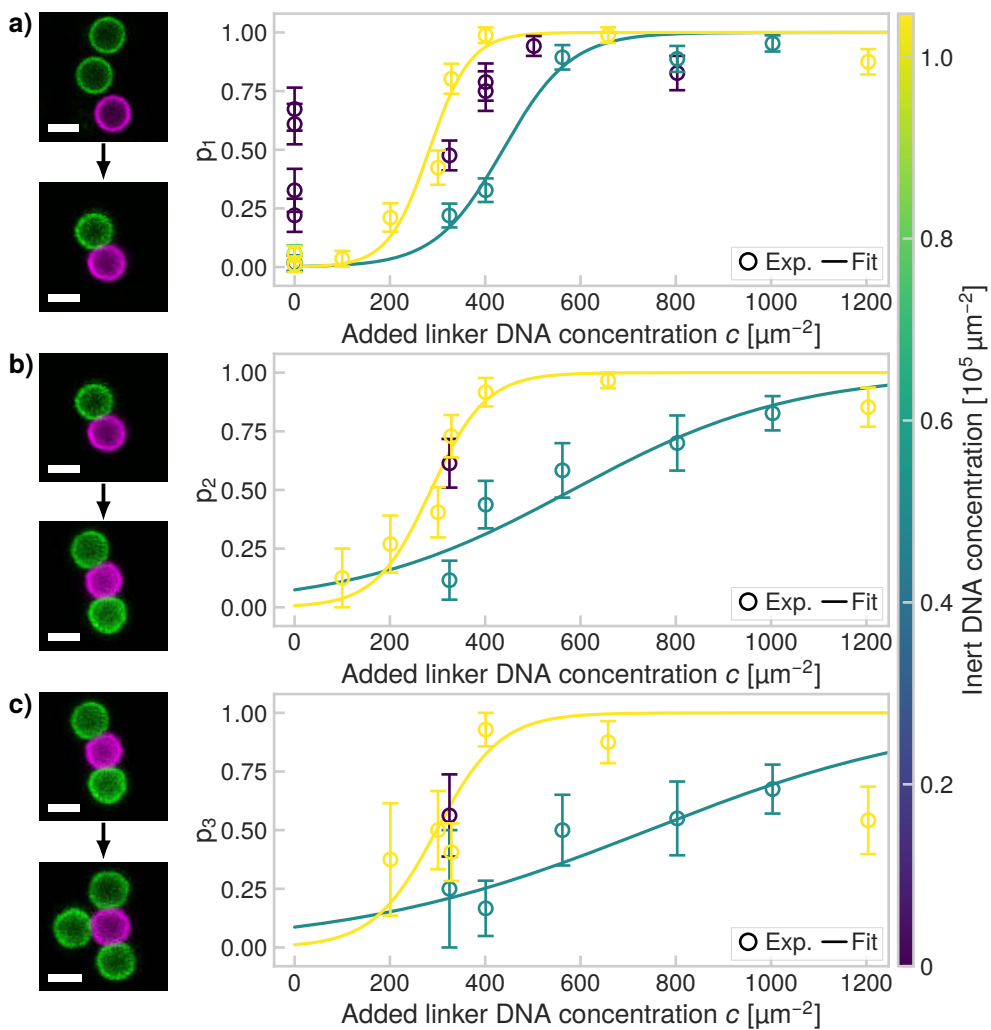
Figure 4.3: **Binding probability of DNA-functionalized CSLBs. a)** First, we have probed the probability p_1 of binding two CSLBs to each other, as depicted in the confocal images. **b)** As shown in the confocal images, for pairs of particles that were successfully bonded, we tried to bind another particle to the central particle (here, in purple) and in that way measured the probability p_2. **c)** In the same way, we determined p_3 by binding an additional particle to a cluster of valency $n = 2$, as shown in the confocal images. Scale bars are 2 µm. In all panels, we have fitted Equation 4.2 to the experimental data.

to analytically model the binding probability of DNA-coated colloids where the effects of linker mobility and linker depletion are simultaneously taken into account. These effects have been studied using numerical simulations[126,229,243] and various analytical expressions were proposed[238,239] for the case that the linkers are grafted on a surface. For DNA-functionalized emulsion droplets[84] a model was proposed that takes the mobility of the linkers into account, but there the deformability of the emulsion droplets played a large role. Unfortunately, these models are not applicable to our system, because the interactions between colloids coated with mobile linkers are not pairwise additive[229] and the CSLBs are not deformable due to the solid support given by the spherical silica particle. Additionally, existing theories assume that the binding and unbinding of the individual DNA linkers is fast, meaning that all the possible binding configurations are sampled equally. This assumption, which states that the system is in thermodynamic equilibrium, may not hold for the current system. Namely, the interactions between sticky ends are expected to be on the order of 2 $k_B T$ (see Figure 4.5 for details) which is higher than the thermal energy and therefore the lifetime of bonds may be too long for equilibrium conditions to apply.

Therefore, to further quantify the observed trends, we have fitted the experimental binding probabilities p_n using a simple logistic model that reproduces the trends in the experimental data,

$$p_n(c) = \frac{1}{1 + \exp\left(-k_n(c - c_{n,0})\right)},$$
(4.2)

where c is the DNA linker concentration in μm^{-2}, k_n is the logistic growth rate for valency n in units of μm^2 and $c_{n,0}$ is the concentration of the midpoint of the binding probability curve of valency n in units of μm^{-2}. The logistic growth rate k_n quantifies the increase in binding probability as function of linker concentration c, where the slope at $c = c_{n,0}$ is given by $p'_n(c_{n,0}) = k_n/4$. $c_{n,0}$ is the DNA linker concentration where $p_n(c_{n,0}) = 1/2$. We stress that Equation 4.2 is not a physical model but an empirical one that we use to quantify the observed trends in the experimental data in the absence of an appropriate analytical model. In future work, we hope to adapt proposed models[229,238] to our experimental system. Such models could improve the accuracy of the measured values we report here, but we find that the simple logistic function we have used here is already sufficient to describe the most important trends in our data.

Indeed, by fitting Equation 4.2 to our experimental data as shown in Figure 4.3, we note that the logistic function can be used to describe the observed dependence on the linker concentration for both concentrations of inert DNA. To quantify the possible effects of linker depletion in greater detail, in Figure 4.4, we show the values of the obtained fit parameters. In Figure 4.4a, we show the concentration c_0 where $p = 0.5$ as function of valency. There, we see an increase of c_0 for the lower inert DNA concentration ($0.5 \times 10^5 \ \mu m^{-2}$), while for the higher inert DNA concentration ($1 \times 10^5 \ \mu m^{-2}$) c_0 is constant. Because of the large uncertainty on c_0, we can not rule out that c_0 is constant for both inert DNA concentrations, but an increase in c_0 would
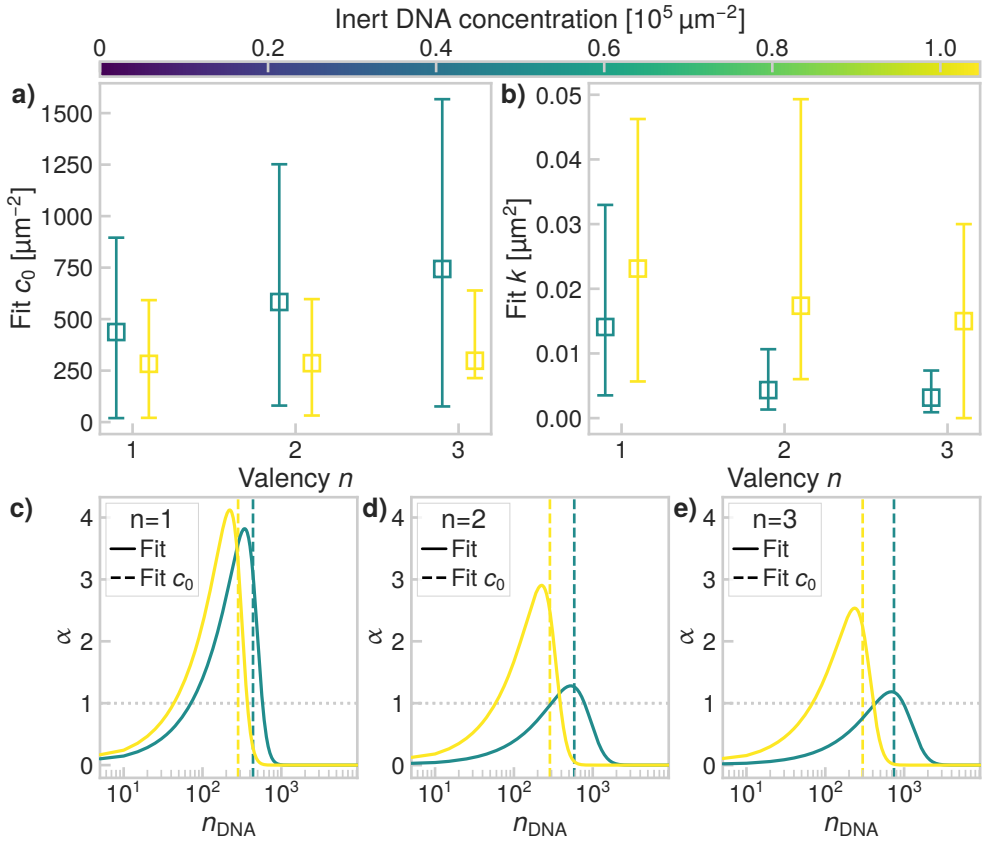
Figure 4.4: **Modeled binding probability as function of valency. a)** The midpoint concentration c_0 increases as function of valency n. **b)** The logistic growth rate k decreases as function of valency n. In panels a and b, the points are slightly displaced along the valency axis for visual separation. **c)** The selectivity α given by Equation 4.3 for valency $n = 1$. For both inert DNA concentrations, the values of α show that the binding is super selective. **d)** The inter-particle selectivity (or affinity) α given by Equation 4.3 for valency $n = 2$. We observe super-selective behavior for the high inert DNA concentration ($1 \times 10^5 \, \mu m^{-2}$), for the lower inert DNA concentration ($0.5 \times 10^5 \, \mu m^{-2}$) the binding is significantly less selective. **e)** The affinity α given by Equation 4.3 for valency $n = 3$. Similarly to panel d, we observe super-selective behavior for the high inert DNA concentration ($1 \times 10^5 \, \mu m^{-2}$), for the lower inert DNA concentration ($0.5 \times 10^5 \, \mu m^{-2}$) the binding is significantly less selective.

also be expected when linkers are depleted as function of valency. We find that the values of c_0 are consistently larger for the lower inert DNA concentration compared to the higher one.

From Figure 4.4b, it can be seen that the logistic growth rate k seems to decrease as function of valency. However, because of the large uncertainty on the fitted values of k, we can not rule out the possibility that k is constant. Nonetheless, these effects taken together suggest that the binding probability shows a complex dependence on both the DNA linker concentration and the inert DNA concentration. Where the binding probability rapidly increases around c_0 for all valencies for the high inert DNA concentration ($1 \times 10^5\ \mu m^{-2}$), as shown in Figure 4.3, the behavior is very different for the lower inert DNA concentration ($0.5 \times 10^5\ \mu m^{-2}$). For the lower inert DNA concentration, for valency $n = 1$ there is a steep increase of p around c_0, but for the higher valencies, the transition is broadened. This suggests that linker depletion also affects the inter-particle selectivity, or affinity, of the interaction.

In our multivalent system, for a certain range of interaction conditions, the dependence of the binding probability on linker concentration can result in super-selective behavior.[238] That is, below a certain threshold of the linker concentration, no binding occurs, while above this concentration threshold, the binding probability rapidly increases,[238] resulting in a step-like binding probability as function of linker concentration. The selectivity, or affinity, of a system can be characterized by the affinity parameter α:[238]

$$\alpha = \frac{d \ln p_n(c)}{d \ln n_{DNA}(c)}. \tag{4.3}$$

Here, n_{DNA} is the number of DNA strands in the binding area of one of the particles, given by[85] $n_{DNA} = 2\pi R_p L_{DNA} c \approx 0.2c$ for our system, where the particle radius $R_p = 1.06\ \mu m$ and the length of the DNA linker $L_{DNA} \approx 30\ nm$. As shown in Figure 4.4c, for valency $n = 1$, the affinity α is greater than one for certain linker concentrations, which indicates that the binding is super-selective for both inert DNA concentrations in that regime. This means that around the threshold concentration, the binding probability will increase as[238] $\propto (n_{DNA})^\alpha$. For valencies $n = 2$ and 3 in Figure 4.4d and e, respectively, we again observe a qualitative difference between the two inert DNA concentrations. For the highest inert DNA concentration ($1 \times 10^5\ \mu m^{-2}$), the affinity of $n = 2$ and 3 is lower with respect to $n = 1$ but still greater than one for a range of linker concentrations, indicating that the behavior is super-selective there. For the lower inert DNA concentration ($0.5 \times 10^5\ \mu m^{-2}$), however, for the higher valencies, the affinity is close to or below one. This indicates a qualitative change in binding behavior for higher valencies for this concentration of inert DNA, where the binding transitions from being super-selective at valency $n = 1$ to a significantly lower affinity at valencies $n = 2, 3$.

To summarize, we have found indications that linker depletion changes the binding probability of DNA linker-functionalized CSLBs. We have tested two different concentrations of inert DNA and find a qualitatively different behavior. For the higher
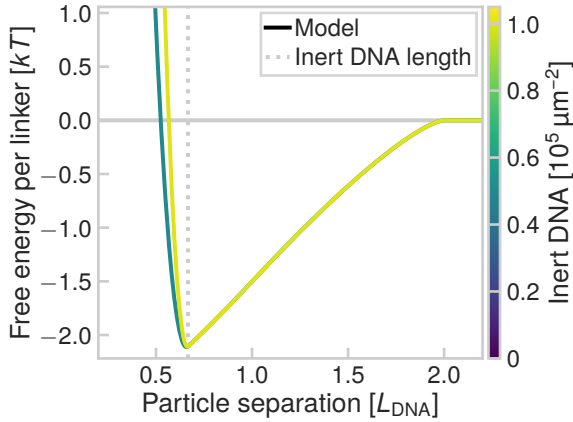
Figure 4.5: **Modeled free energy for grafted linkers based on a mean-field approach.**
We used the code made available in the Python package `DNACC`.[239,247,248] We set the
hybridization free energy of the linkers to $-15.5k_BT$ as calculated from the DNA
sequence of the single stranded sticky end.[249] This neglects other contributions to
the hybridization free energy stemming from the rest of the linker, which is a double-
stranded DNA complex with a hydrophobic anchor. For a linker density of $350\,\mu m^{-2}$,
close to the midpoint concentrations c_0, we observe only small differences between
the two inert DNA concentrations used here.

inert DNA concentration, the effect of linker depletion is more subtle: there is only
a slight broadening and shift of the binding probability as function of valency and
the binding is super-selective for all three valencies that we tested. In contrast, for
the lower inert DNA concentration, the transition in binding probability shifts to-
wards higher DNA concentrations as function of valency, the transition broadens as
function of valency and for valencies $n = 2, 3$ we find that the binding is no longer
super-selective.

It is unclear how to explain the complex behavior that we have found in our
experiments. Because the inert DNA strands ($\approx 20\,nm$) are shorter than the linker
DNA strands ($\approx 30\,nm$), it is unlikely that the interaction potential is significantly
altered as function of inert DNA concentration, as these strands only provide a
short-range repulsive component that should in principle not affect the binding of
the linkers. We have checked this hypothesis by following the mean-field approach
described by Varilly et al.[239] and Angioletti-Uberti et al.[248] using the Python package
`DNACC`[247] and found that indeed, as shown in Figure 4.5, the interaction potential is
not significantly changed by comparing the two inert DNA concentrations at the same
linker concentration of $350\,\mu m^{-2}$. Although in these models, linker mobility is not
taken into account, this calculation suggests that the relative sizes and concentrations
of the inert DNA and linker DNA are not sufficient to explain the observed behavior.
However, we note that it is possible that other effects also influence the interaction

potential, such as excluded volume interactions between linker DNA and inert DNA.

Moreover, we hypothesize that multiple effects could simultaneously contribute to the observed trends in the experimental data. First, the actual DNA concentration on the particles is not known. We have assumed here that all the DNA strands that are added in solution are actually inserted into the bilayer on the particles, which is probably not the case. Previous measurements of the DNA linker concentration showed a large spread in the linker concentration across different particles in the same sample.[85] Such a large spread would lead to a broadening of the measured binding probability curves.

Second, the fraction of DNA linkers that are inserted into the bilayer could be affected by the relative concentrations of inert and linker DNA strands. Because of the hydrophobic anchors that are attached to the hydrophilic DNA strands, the DNA complexes could form micelles in solution depending on their concentration. This could lead to a balance between the DNA complexes that are inserted into the lipid bilayer and the DNA complexes that form micelles. This, in turn, is then affected by the total concentration of inert and linker DNA, which could result in different linker DNA coating densities at different inert DNA concentrations. However, the critical micelle concentration of these complexes is not currently known.

Similarly, the competition between linker DNA and inert DNA strands to insert into the lipid membranes could lead to lower concentrations of linker DNA inserted into the CSLBs at higher inert DNA concentrations. Interestingly, our experimental results seem to contradict this hypothesis, as the fitted c_0 for the higher inert DNA concentration is lower than that of the lower inert DNA concentration, which hints at a higher average DNA linker density for the higher inert DNA concentration.

Finally, the observed trends with increasing valency are hard to interpret because the sticky ends we have used are not permanently bonded at room temperature, as the average free energy per sticky end is at most on the order of a few $k_B T$, as shown in Figure 4.5. Therefore, the number of linkers in the binding patch area may not be constant in time and there could be a redistribution of linkers as function of valency.

In conclusion, the DNA linker-mediated interactions we have measured here constitute a complicated and dynamic system. To explain the observed experimental trends, more research is needed both on the experimental and theoretical aspects of multivalent interactions of mobile linkers.

4.3.2 Application to self-assembly experiments

We have characterized the experimental binding probability as function of DNA linker concentration for valencies up to three. Next, we can use these results to calculate the combined probability to form clusters of a specific valency up to $n = 3$. We do so by defining the total probability $p_{\text{tot.}}(n, c)$, which is the product of the binding probabilities of valencies up to n as given by

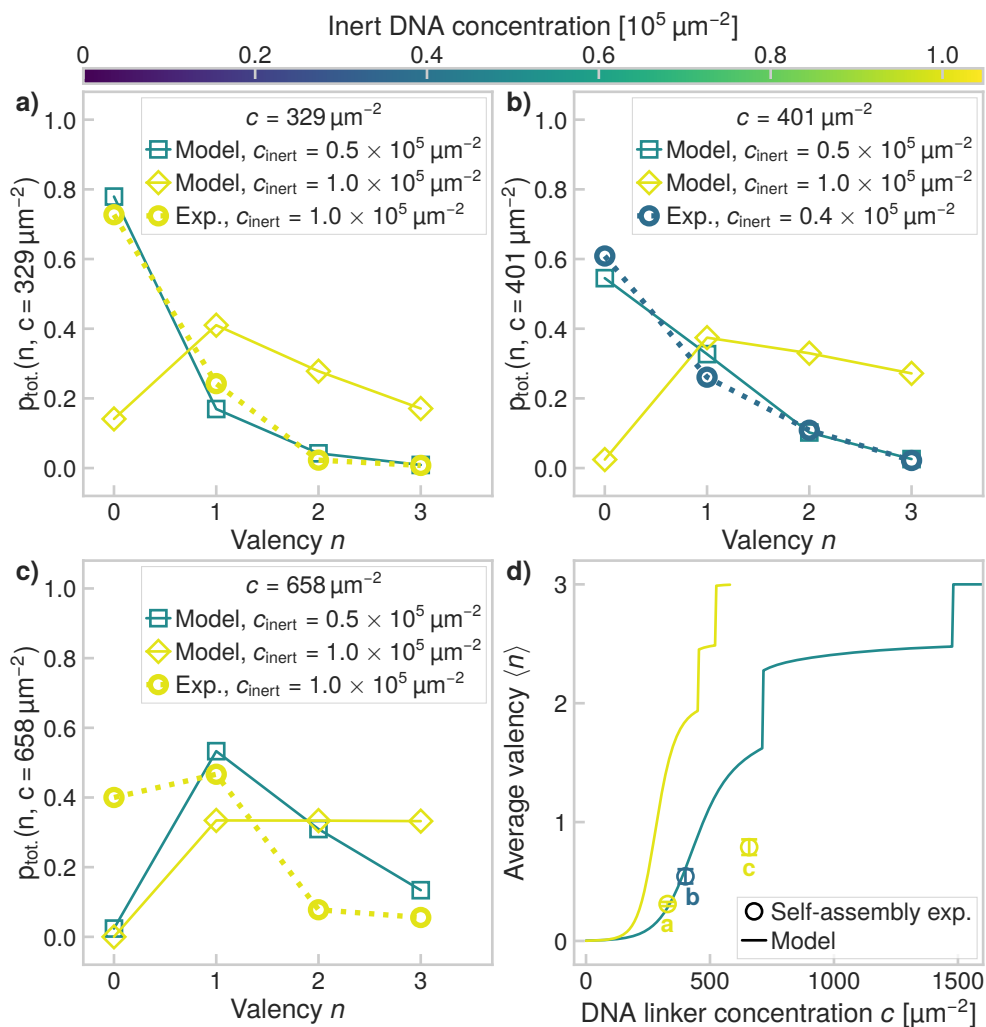$$p_{\text{tot.}}(n, c) = \prod_{i=1}^{n} p_n(c). \tag{4.4}$$

Figure 4.6: **Expected average valency as function of DNA linker and inert concentration.** In panels a-c, we show the cumulative binding probability $p_{tot.}$ based on Equation 4.4 for the DNA linker concentrations used in the self-assembly experiments shown here. In all cases, the experimental distributions are close to the obtained distributions for the lower inert DNA concentration $c_{inert} = 0.5 \times 10^5\,\mu m^{-2}$. **a)** $p_{tot.}$ for $329\,\mu m^{-2}$ DNA linkers. **b)** $p_{tot.}$ for $401\,\mu m^{-2}$ DNA linkers. **c)** $p_{tot.}$ for $658\,\mu m^{-2}$ DNA linkers. **d)** The expected average valency as function of the initially added DNA linker concentration and inert DNA concentration (color), as calculated from Equation 4.5. Experimentally determined values from self-assembly experiments corresponding to panels a-c are indicated as well.

For a valency equal to zero, $p_{\text{tot.}}(0, c) = 1 - \sum_{i=1}^{n} p_{\text{tot.}}(i, c)$. This cumulative binding probability $p_{\text{tot.}}$ gives an upper bound on the expected valency that can be found in self-assembly experiments.

We test the predictive power of the cumulative binding probability determined from optical tweezers experiments, by performing three different self-assembly experiments, as explained in Section 4.2.3. Briefly, we have used two sets of CSLBs functionalized with complementary DNA linkers at a high number ratio of 1:30 to drive the self-assembly process towards the formation of clusters,[85] as opposed to other structures such as chains and fractal aggregates. We show the average valency for three different DNA concentrations, where the average valency was measured after at least 24 h of mixing. In Figure 4.6a-c, we show the cumulative probability for three different DNA linker concentrations used in the self-assembly experiments.

First, we consider the experiment that uses a lower inert DNA concentration, as shown in Figure 4.6b. For that combination of inert and linker DNA concentrations, as determined from Figure 4.3, the binding probability is on the order of 0.5 for $n = 1$ and significantly lower for valencies $n = 2, 3$. This implies that because of the low probability to form a duplex when two particles briefly come into close contact, the assembly process is dominated by the binding probability. Indeed, we observe good agreement between the expected and measured valency distributions in Figure 4.6b.

Second, we have performed two experiments where the inert DNA concentration was higher, as shown in Figure 4.6a and c. Starting with the experiment in Figure 4.6a, we note that for those combinations of inert and linker DNA concentrations, the expected binding probability determined from Figure 4.3 is larger than or equal to 0.5 for all three valencies. However, we find a lower average valency than would be expected from Equation 4.4. Perhaps coincidentally, the observed valency distribution coincides with the distribution predicted for the lower inert DNA concentration. For the third experiment shown in Figure 4.6c, which uses the same higher inert DNA concentration as the experiment in panel a, we observe the same: a lower than expected average valency and a distribution that seems to coincide with the distribution predicted for the lower inert DNA concentration. There could be several explanations for these observations. First, due to variations between experiments, it is possible that the actual inert DNA concentration on the particles is lower than expected. Second, other experimental factors than the binding probability alone could have led to a slower self-assembly process, such as particles that stick to the substrate or contamination of the samples by DNase enzymes, that reduce the effective concentrations of intact inert and linker DNA on the particles. While we have tried to mitigate these effects as much as possible, more experiments are needed to fully test our hypothesis.

In addition to the distribution of observed valencies, we can calculate the average valency $\langle n \rangle$, as shown in Figure 4.6d. For the experimental data, it can be seen that by tuning the DNA linker concentration, the expected average valency $\langle n \rangle$ can be tuned. We have compared the experimental average valency to our predictions by calculating the average valency based on the expected distributions of n, as shown

for a few linker concentrations in Figure 4.6a-c. We determined $\langle n \rangle$ as follows

$$\langle n \rangle = \left(\sum\nolimits_{\substack{i=0 \\ p_{\text{tot.}} \leq 0.99}}^{n} p_{\text{tot.}}(i,c)\, i \right) / \sum\nolimits_{\substack{i=0 \\ p_{\text{tot.}} \leq 0.99}}^{n} p_{\text{tot.}}(i,c), \qquad (4.5)$$

where we used a probability of 0.99 as a cutoff value, above which we considered the binding probability to be equal to unity. In Figure 4.6d, we show the full dependency of the expected average valency on the added DNA linker concentration, up to a maximum valency of three, which is the maximum valency that we have measured both using the optical tweezers method and in these self-assembly experiments. Again, we note that the limited experimental data that is available seems to show a similar trend, in spite of differences in inert DNA concentration that would result in very different binding probabilities and therefore, average valencies, as plotted in Figure 4.6d. In an upcoming work,[250] we will study the self-assembly of these types of colloidal clusters in greater detail.

In conclusion, the experimental data shows a qualitatively similar trend as the predicted average valency for low linker concentrations. For the experimental data where the inert DNA concentration is high ($1 \times 10^5\ \mu\text{m}^{-2}$) in Figure 4.6a and c, the experimental distributions are closer to the expected distributions of the low inert DNA concentration ($1 \times 10^5\ \mu\text{m}^{-2}$). As discussed, more experiments are necessary to fully test how the total binding probability predicted by Equation 4.4 compares to the experimentally observed valencies in self-assembly experiments.

Based on our preliminary data, we conclude that the linker concentration can be used to tune the average valency of colloidal clusters in self-assembly experiments. We have exploited this dependence of the average valency on DNA linker concentration in chapters 5 and 6, where we assembled flexible colloidal chains using low linker concentrations, that ensured an average valency close to two. In future experiments, we plan to repeat these self-assembly experiments for a larger range of DNA linker concentrations in order to further test our predictions.

4.4 Conclusions

In this chapter, we have used optical tweezers to directly probe the binding probability of DNA-decorated colloid-supported lipid bilayers as function of DNA linker concentration and valency. First, we have determined the optimal parameters to provide colloidal stability. We have found that a total DNA concentration above approximately $10^4\ \mu\text{m}^{-2}$ is sufficient to completely suppress nonspecific aggregation. In addition, we have shown that both linker and inert DNA complexes can be used to provide colloidal stability. Then, we have characterized the binding probability as function of DNA linker concentration and valency in terms of a simple model given by a logistic function. We have found a complex dependence on inert DNA concentration and linker DNA concentration as function of valency and conclude that more research is needed to explain these effects in terms of a physical model. Our results indicate that linker depletion effects as function of valency lead to a decrease in the

binding probability. We have shown that by varying the DNA linker concentration, the average valency of colloidal clusters can be tuned in self-assembly experiments.

Linker depletion presents a promising way to control the average valency in self-assembly experiments. The mechanism could be used to fabricate structures of the desired geometry, such as clusters of valency four, that are believed to be able to crystallize into diamond lattices that have interesting photonic properties.[59,71] The fact that CSLBs are reconfigurable due to their flexible bonds, could lead to applications in switchable materials. Beyond applications for colloidal self-assembly processes, our findings could have implications for multivalent interactions found in biological systems, such as in cell-signaling and drug-delivery systems.